



HAL
open science

Fully inkjet printed SnO₂ gas sensor on plastic substrate

Mathilde Rieu, Malick Camara, Guy Tournier, Jean-Paul Viricelle, Christophe Pijolat, Nicolaas F de Rooij, Danick Briand, J.P. Viricelle

► To cite this version:

Mathilde Rieu, Malick Camara, Guy Tournier, Jean-Paul Viricelle, Christophe Pijolat, et al.. Fully inkjet printed SnO₂ gas sensor on plastic substrate. *Sensors and Actuators B: Chemical*, 2016, 236, pp.1091-1097. 10.1016/j.snb.2016.06.042 . hal-01330977

HAL Id: hal-01330977

<https://hal.science/hal-01330977>

Submitted on 26 Aug 2016

HAL is a multi-disciplinary open access archive for the deposit and dissemination of scientific research documents, whether they are published or not. The documents may come from teaching and research institutions in France or abroad, or from public or private research centers.

L'archive ouverte pluridisciplinaire **HAL**, est destinée au dépôt et à la diffusion de documents scientifiques de niveau recherche, publiés ou non, émanant des établissements d'enseignement et de recherche français ou étrangers, des laboratoires publics ou privés.

Fully inkjet printed SnO₂ gas sensor on plastic substrate

Mathilde Rieu^{a,*}, Malick Camara^b, Guy Tournier^a, Jean-Paul Viricelle^a, Christophe Pijolat^a, Nico F. de Rooij^b, Danick Briand^b

^a École Nationale Supérieure des Mines, SPIN-EMSE, PRESSIC, CNRS:UMR5307, LGF, F-42023 Saint-Étienne, France

^b Ecole Polytechnique Fédérale de Lausanne (EPFL), Institute of Microengineering (IMT), Sensors, Actuators and Microsystems Laboratory (SAMLAB), Rue de la Maladière 71b, 2000 Neuchâtel, Switzerland

* Corresponding author: M. Rieu. Tel.: +33 4 77 42 02 82; fax: +33 4 77 49 96 94. E-mail address: rieu@emse.fr

Abstract

A tin dioxide (SnO₂) sensor was fabricated by inkjet printing onto polyimide foil. Gold electrodes and heater were printed on each side of the substrate. A SnO₂ based ink was developed by sol-gel method and jetted onto the electrodes. A final annealing at 400°C compatible with the polymeric transducers allowed to synthesize the SnO₂ sensing film. Electrical measurements were carried out to characterize the response of the fully printed sensors under oxidizing and reducing gases. The device was heated up at a temperature between 200 and 300°C using the integrated heater. The proper operation of the full printed metal-oxide gas sensors was validated under exposure to carbon monoxide and nitrogen dioxide, in dry and wet air.

Keywords

SnO₂ sensor; Sol-gel synthesis; Inkjet printing; Polyimide foil; Gold heater

Highlights

The whole gas sensor was prepared by inkjet printing technology on a polymeric foil. Sol-gel synthesis allowed to obtain crystallized SnO₂ film at a temperature of 400°C. The sensor processing is compatible with the use of polyimide substrate.

1. Introduction

Development of sensing devices onto flexible foils is receiving special attention with the advances made in printed electronics [1-4]. Indeed, the development of sensors on plastic substrates is of growing interest, with the aims of achieving low-cost, flexible, and wireless devices [5].

Compared to silicon technology, fabrication on plastic substrates can simplify sensors manufacturing by avoiding bulk micromachining and high temperature process steps required, for instance, in the realization of silicon micro-hotplates. However, it demands the development of material synthesis and deposition procedures compatible with the temperature plastic supports.

Previous work reporting on the realization of metal-oxide gas sensors onto plastic substrate is based on clean room fabrication processes [6-7]. Nowadays, additive manufacturing using printing is of interest to reduce the infrastructure and simplify the sensors fabrication procedure. Among the different printing techniques, ink-jet printing is a contactless technique able to deliver digitally precise quantities of materials to form well-defined patterns. This technique is used for the preparation of different functional films [1, 8-11].

Until now, inkjet printed hotplates on polymeric foil were limited to an operating temperature of about 100°C due to the use of silver ink [9-10]. However, metal-oxide gas sensors normally require higher operating temperatures and more inert materials, such as gold or platinum, must be implemented.

Regarding inkjet printing of metal-oxide sensing layers, the works published deal with the deposition onto rigid substrates, made of silicon or alumina [12-15]. The ink can be composed of either precursors or nanoparticles to prepare the oxide film, but the sintering step occurred at more than 500°C, which is not compatible with the use of plastic foil.

We report here on the preparation and the characterization of fully inkjet printed SnO₂ sensors with integrated heater onto polyimide (PI) film able to operate at temperatures up to at least 300°C. The hotplate transducers were made of inkjet printed gold electrodes and heater. SnO₂ was chosen as gas sensitive layer as it has been widely used as gas-sensing material since

many years and plays a central role in the field of gas sensors [16-19]. A custom made ink of tin oxide was formulated and its synthesis using a sol-gel process was studied. The gold transducers on polyimide foil were coated via inkjet printing with the custom made ink solution and, finally, the electrical response of the sensor to different gases was characterized.

2. Experimental

2.1. Substrate preparation

A flexible foil was used as substrate. Polyimide (PI) Upilex-50S, 50 μm in thickness, was selected because of its heat resistance property, with the capability of preserving its physical and chemical properties at high temperature (up to 500°C). Prior to the printing step, the substrate was cleaned by successive immersion in acetone, isopropanol and deionized water. After the cleaning process, it was dried into an oven at 120°C for 1h. The substrate could be optionally subjected to an oxygen plasma treatment (Diener Zepto Plasma reactor) for 2 min at 100 W (40 kHz) to modify its surface energy.

2.2. Design and printing of the sensors

The transducer consists of gold electrodes on one side of the PI foil and of a gold heater on the other side as shown in Figure 1. Electrodes were designed to have a simple two parallel lines structure (Fig.1 b). The design of the heater (Fig. 1 c) was not optimized to minimize the power consumption of the device but to achieve a high printing yield.

Commercial gold ink (NPG-J from Harima) was ink jetted onto the PI substrate. The printer used was a Dimatix DMP-2800 with 10 pL cartridges. After printing, gold coatings were placed in an oven at 250°C for 3 hours to sinter the ink.

SnO_2 ink was then deposited onto the electrodes. The shape of the sensing element was a rectangle of 4 x 2 mm^2 in order to fully cover the electrodes and the space in between.

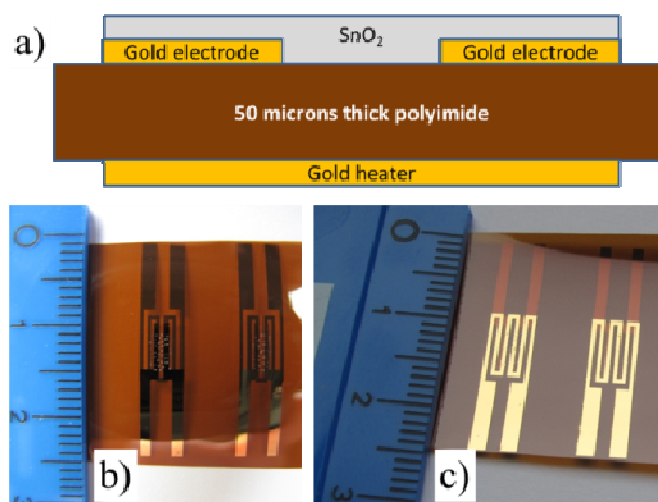


Fig. 1. Cross section schematic view of the device (a) and photographs of the top side (electrodes and SnO₂) of the device (b) and of the back side (heater) (c).

2.3. SnO₂ ink preparation

The SnO₂ material was prepared using sol-gel process as described in the literature [20-22]. SnCl₂ was dissolved in pure ethanol with a concentration of 0.25 mol.L⁻¹. The mixture was stirred and kept at 80°C for 5 h in a closed vessel to form a transparent tin ethoxide solution (Sn(OEt)₂). The obtained sol was clear and homogeneous. Furthermore, the sol was stored in a closed vessel and was stable over some months if keeping out of contact of humidity.

To inkjet the sol, viscosity and surface tension have to be adjusted to fulfil the requirements of the inkjet printer. For the printer used, the range of viscosity and surface tension are 10-12 mPa.s and 30-35 mN.m⁻¹, respectively. Inks viscosity and surface tension measurements were carried out with a viscosimeter DV-II+ by Brookfield and a portable tensiometer AquaPi by Kibron, respectively.

Sol viscosity was 1.5 mPa.s and its surface tension was 22 mN.m⁻¹. In order to adjust these properties, ethylene glycol (EG) was added to the sol. Ethylene glycol was chosen because of its boiling temperature point near 200°C, which is higher than the 100°C recommended for inkjet printing in order to prevent quick evaporation and blocking of the nozzle. By adding EG to the sol, viscosity and surface tension were increased. Various amounts of sol and EG were mixed. The solution that fulfil the best the requirements of the inkjet printer was composed of 25 vol% of sol and 75 vol% EG with a viscosity of 10.2 mPa.s and surface tension of 35 mN.m⁻¹.

The SnO₂ ink was then put into a cartridge. Dimatix software was used to set the printing parameters. The jetting waveform used for the deposit was adapted from a model given into the Waveform Editor software of the printer, with a firing voltage set at 20V and a cartridge temperature fixed at 30°C.

2.4. Characterization techniques

Thermal analyses of the xerogel, thermo-gravimetric analysis (TGA) and differential scanning calorimetry (DSC), were performed with a coupled TGA/DSC Star^eSystem from Mettler Toledo. Analyses were performed from room temperature to 800°C under 5 L h⁻¹ air flow.

X-ray diffraction (XRD) analysis was performed onto powder with a Siemens D5000 diffractometer using Cu K α radiation at 40 kV and 40 mA. Environmental scanning electron microscopy (ESEM Philips 30XL ESEM-FEG) was used to investigate the surface morphology of the coatings. Transmission Electron Microscopy (TEM Philips CM 2000) was used to characterize the SnO₂ powder and the cross section of the sensor. In order to prepare the sensor's cross section, the lamella was prepared using a Focus Ion Beam (FIB) equipment (Equipex MANUTECH-USD). Carbon and platinum were deposited on the top of the SnO₂ layer during the preparation of the lamella.

The gas sensing performances of the sensors were evaluated thanks to a gas mixing system equipped with mass flow controllers. Carbon monoxide and nitrogen dioxide, gases representative of atmospheric pollution field, were used as reducing and oxidizing gases, respectively. It was possible to generate concentrations from 1 to 50 ppm of CO and from 0.6 to 20 ppm of NO₂, either in dry air or wet air (1 vol % absolute humidity, which corresponds to 50% relative humidity at 20°C) as carrier gas. The sensor was put in a cell exposed to a constant gas flow of 10 L h⁻¹. Thanks to a power supply, the gold heater at the backside of the sensor allowed to heat up the tin dioxide material between 200 and 300°C. The electrical responses of the sensors were measured using a multimeter (HP 34410A). Resistance data were recorded as a function of time. Chemo-resistive gas responses, defined as $R_{\text{air}}/R_{\text{CO}}$ or $R_{\text{NO}_2}/R_{\text{air}}$, of the sensor under dry and wet air were calculated to compare the printed sensors characteristics to those of sensors reported in the literature. The chemo-resistive responses mean value of two tested devices and the standard deviations were calculated and used to plot calibration curves. The limit of detection (LOD) was also calculated and is defined as 3 times

the standard deviation of the background noise. Unfortunately, sensors electrical responses to NO_2 injections of 5 and 20ppm were not measurable at 200°C (out of range $R > 10^8$ ohm).

3. Results and discussion

3.1. Characterization of SnO_2 precursor

Before establishing the inkjet printing process of the solution, the sol was hydrolyzed to obtain a gel in order to characterize it. By adding water (50 vol %) to the sol and letting the mixture 24h into a close bottle vessel at 80°C -4h in an oven, the transformation sol to gel occurred. The inorganic network of the gel retains a large amount of liquid phase composed of water and organic solvent. This gel was then dried at 80°C for 24h to obtain a xerogel. Changing from a humid gel to dry xerogel powder, the major part of the liquid phase was removed. Then, the decomposition in air of the xerogel was investigated by thermogravimetric analysis (TGA) and differential scanning calorimetry (DSC). Weight loss and heat flow are reported as a function of the temperature in Fig. 2.

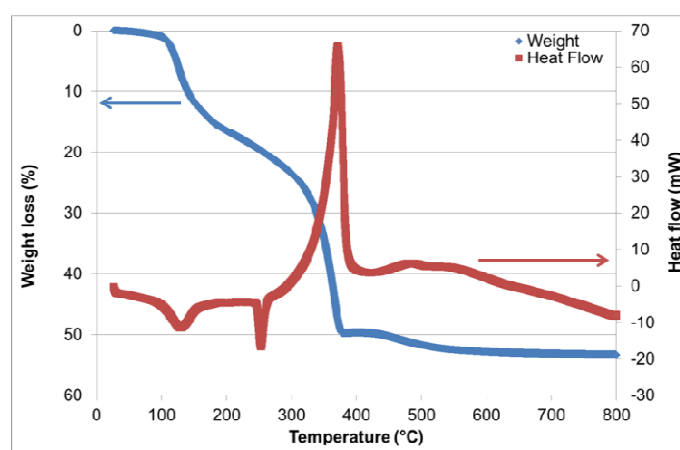


Fig. 2. Thermo-gravimetric analysis (weight loss) and differential scanning calorimetry (heat flow) of SnO_2 xerogel as a function of the temperature.

The TGA curve shows, with increasing temperature, a continuing loss of mass linked to the decomposition of the organic compounds retained by the inorganic network of the xerogel. Around 400°C , the total loss of weight constitutes 50 wt % of the initial xerogel weight. The shape of the DSC curve indicates endothermic effects in the low temperature range (20-

300°C), which are most frequently attributed to organics decomposition. At 375°C, a sharp exothermic process occurs simultaneously with the highest weight loss. As crystallization process is generally associated with an exothermic peak, this can be associated to SnO₂ crystallization [23, 24].

To confirm the crystallization of the compound at around 400°C, X Ray Diffraction (XRD) analysis was done onto SnO₂ powder annealed at 400°C-1h. The powder was crystallized in the tetragonal structure of SnO₂. The average crystallites size was calculated using Scherrer equation and was 11 ± 1 nm. The average crystallite size was confirmed by transmission electron microscopy (TEM) done on the powder annealed at 400°C. Indeed, as it can be observed on the micrograph reported in Fig. 3, the SnO₂ powder is composed of crystallites of around 10 nm of diameter. These crystallites are agglomerated into larger particles.

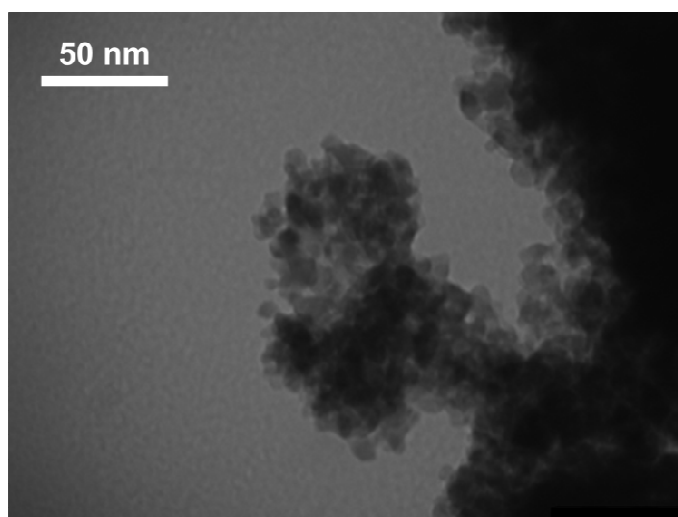


Fig. 3. TEM micrograph of the SnO₂ powder after annealing at 400°C-1h.

3.2. Inkjet printing of the whole sensor onto polyimide substrate

3.2.1. Printing gold transducers

A commercial gold ink was printed to pattern the electrodes and heater onto cleaned and dried PI foil without further surface treatment. The inkjetted spots exhibited a diameter of around 150µm. Thus, a drop to drop spacing of 100 µm was chosen to obtain a uniform gold layer. Three layers were successively deposited in order to get an electrically conductive track. Gold electrodes were first printed on one side of the PI foil and annealed at 250°C for 3h. The

heater was then printed on the other side of the substrate and sintered also at 250°C-3h. Pictures of electrodes and heater are reported in Fig. 1 b) and c), respectively. The resistance of the heater at room temperature (22°C) was 39 Ω . Its temperature coefficient resistance (TCR) was measured between 20 and 200°C thanks to a climatic chamber. The TCR of the printed gold layer was of $2.0 \cdot 10^{-3} \text{ K}^{-1}$ and was used to set the temperature of the sensor when injecting power into the heater.

3.2.2. *SnO₂ ink deposition*

The reservoir of the printhead was filled with the SnO₂ ink and inkjet printer parameters (cartridge temperature, jetting waveform) were adjusted in order to obtain a drop without satellite.

Then, the effect of the surface treatment of the substrate and of the drop to drop space (DDS) on the printing pattern was evaluated. As reported in Figures 4 a) and c), without a surface treatment of the PI film, the deposited drops were around 30-40 μm in diameter; in this case, a drop to drop space of 20 μm was necessary to get a good coverage of the surface (Fig. 4 c). When performing an oxygen plasma treatment onto the PI surface (Fig. 4 b and d), the deposited drops were spread out with a diameter of 160 μm and a drop to drop space of 100 μm was sufficient to get the coverage (Fig. 4 b). However, the amount of deposited matter was very low in this last case, so making it difficult to see the deposited films as they were almost transparent. Finally, the parameters used for the preparation of the sensor were no surface treatment (only cleaning) and a DDS of 20 μm in order to have a continuous visible deposit (Fig. 4 c).

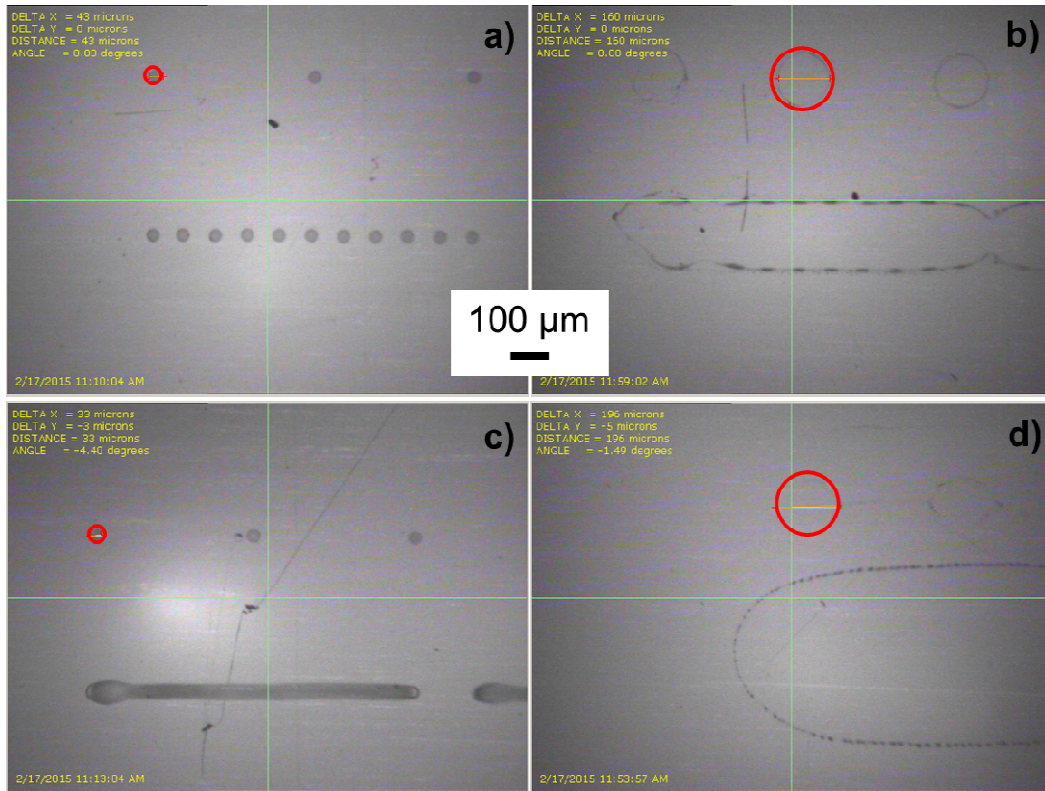


Fig. 4. Optical micrographs of the SnO₂ sol drop deposited onto PI substrate: a) and c) without surface treatment of the substrate, drop to drop spaced of 100 μm and 20 μm , respectively; b) and d) with O₂ plasma treatment of the substrate, drop to drop spaced of 100 μm and 20 μm , respectively. Red circles underline deposited drop size.

To complete the sensor preparation, the SnO₂ ink was printed onto the substrate and the gold electrodes. Four layers were deposited in order to get a visible layer of SnO₂ material. A dry step at 50°C-30 min was implemented between each printed layer. Finally, a thermal annealing at 400°C-1h was applied to form the SnO₂ film.

3.3. Microstructural characterization of the sensing layer

After annealing, the coating was transparent and difficult to observe. SEM micrograph of the sensor is reported in Fig 5. The PI substrate under the active layers is black on the micrograph. The two gold electrodes in grey in the micrograph are 500 μm -wide and spaced by 600 μm . In between the gold electrodes, the SnO₂ coating was transparent (black color) except where the material got accumulated, which resulted in the grey spots shown in Figure 5. Therefore the SnO₂ coating was not homogeneous with some non-transparent amounts of matter locally accumulated.

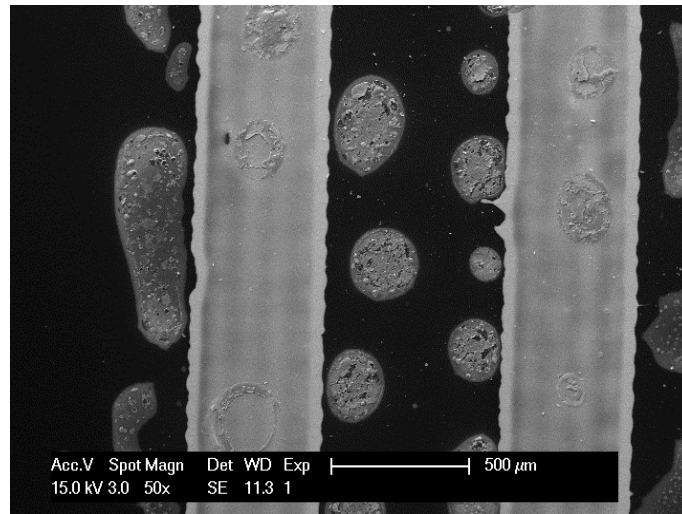


Fig. 5. SEM micrograph of the sensor. The two grey parallel lines correspond to the gold electrodes and the grey dots correspond to SnO₂ accumulation.

The cross section of the sensor was then characterised by TEM analysis, in the area where the transparent coating was located, which means between the two gold electrodes and the grey spots. For this, the lamella was cut thanks to a FIB equipment. The PI substrate and the thin SnO₂ layer can be seen in the micrographs presented in Fig. 6. The SnO₂ layer thickness was determined to be between 10 and 15 nm, which means that this transparent coating is made of only a monolayer of SnO₂ crystallites.

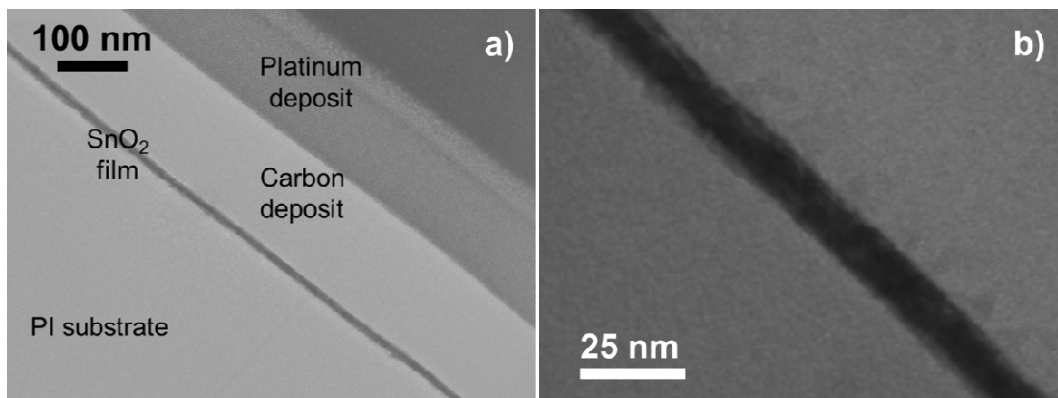


Fig. 6. TEM micrographs of the cross section of the sensor, a) overview and b) SnO₂ layer at higher magnification. Carbon and platinum layers were deposited during the lamella preparation with FIB technique.

3.4. Evaluation of gas sensing performances

Finally, the electrical responses of the sensor under gas exposure were evaluated. The integrated heater at the back side was used to adjust the sensors temperature. A power supply of 0.59 Watt and 0.26 Watt was necessary to heat the sensor up to 300°C and 200°C, respectively. Temperature homogeneity was checked thanks to a K-type thermocouple and a difference of less than 20°C was found all over the sensing element zone which was acceptable. Two sensors prepared using the same procedure were tested and led to the same results. Furthermore, the sensors were tested for more than 30 days with the observation of a slight drift of their baseline but the amplitude of the sensor response remained the same.

Several gas concentrations of CO and NO₂ were injected, either using dry or wet air as carrier gas. The electrical conductance of the sensor versus time is plotted in Fig. 7, with injections of CO and NO₂ in dry air, at 300°C (Fig. 7 a); 200°C (Fig. 7 b) and in humid air at 300°C (Fig.7.c). Under dry air, one can notice that the pure SnO₂ sensor responds to the gases even at low concentrations, such as 1 ppm CO and 0.6 ppm NO₂. Obviously, the reaction kinetics are slower at 200°C compared to 300°C, which implies longer response time and longer recovery time at 200°C. Comparing dry and wet atmosphere, at 300°C (Fig. 7. a) and c)), the main difference is in the baseline. Indeed, water is known to increase the conductance [25]. That also implies that the responses to low concentration of CO are largely hidden in the case of wet air.

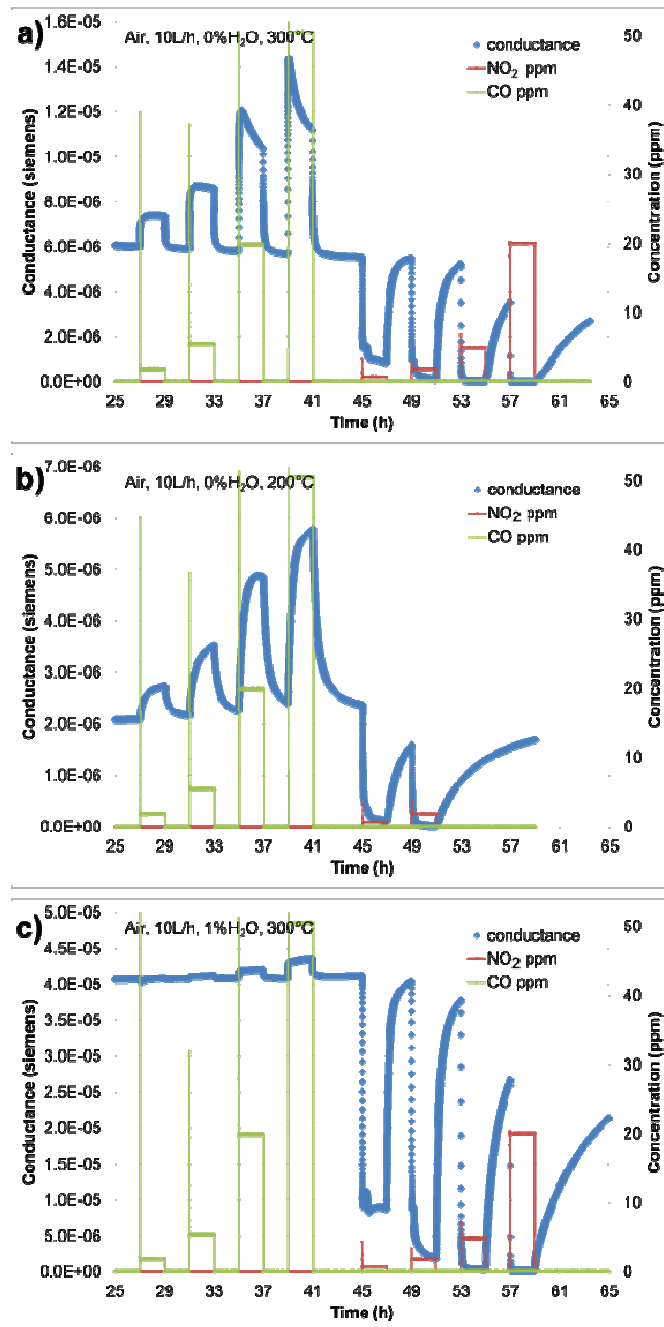


Fig. 7. Evolution of SnO₂ electrical conductance with CO and NO₂ injections at operating temperatures of a) 300°C and b) 200°C in dry air; c) at 300°C in wet air.

Chemo-resistive gas responses ($R_{\text{air}}/R_{\text{CO}}$ or $R_{\text{NO}_2}/R_{\text{air}}$) of the sensor under dry and wet air were extracted from these measurements and were plotted versus gas concentration in Fig. 8. These calibration curves evidence that the presence of the humidity drastically reduced the sensor response to CO gas (Fig. 8.a). Responses were smaller under wet air, nearly divided by 2. In the case of NO₂ (Fig. 8.b), the presence of humidity reduced also the responses but they were still visible. The influence of temperature was less pronounced than humidity effect. The

chemo-resistive responses at 300°C were slightly lower than at 200°C but lowering the temperature affected mainly the kinetics as mentioned previously. Finally, the responses to CO and NO₂ in the investigated temperature range were comparable to result reported in literature for SnO₂ sensors [6, 12, 26]. Under humid atmosphere and for both tested temperatures, 20 ppm of CO was the lowest concentration to obtain exploitable responses of the sensor compared to 0.6 ppm for NO₂.

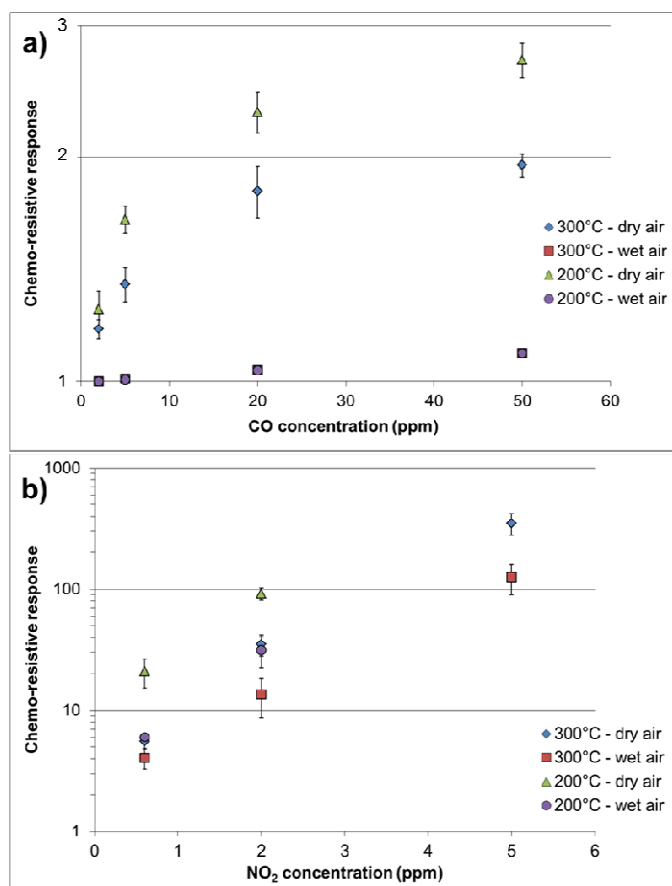


Fig. 8. Calibration curves for CO and NO₂. The chemo-resistive responses ($R_{\text{air}}/R_{\text{CO}}$ or $R_{\text{NO}_2}/R_{\text{air}}$) are the mean value of the two tested sensors and error bars represent the standard deviation.

Limits of detection (LOD) were also calculated and are reported in Table 1. It confirms that the performances of pure SnO₂ are weaker under humid atmosphere than in dry air especially for CO injections. For example, at 300°C, under dry air, less than 1 ppm CO would be detectable while under wet air LOD was higher than 20 ppm. The LOD for NO₂ injections were quite low, a few ppb, which is agreement with literature data [27].

Table 1. Limits of detection of CO and NO₂ of the SnO₂ inkjet printed sensors.

Limit of detection	300°C dry air	300°C wet air	200°C dry air	200°C wet air
CO (ppm)	0.5	24	0.4	46
NO ₂ (ppb)	6	9	1	6

Conclusions

We have demonstrated the first fully inkjet printed metal-oxide sensor onto polymeric foil, including the gas sensitive layer and heating transducer. The reported technology allows the simple preparation of tin oxide sensors with results comparable to what has been published so far in the literature on this type of sensors. We have reported on a sol-gel tin oxide film compatible with inkjet printing and the use of a polyimide substrate thanks to its synthesis temperature of 400°C. The different fabrication steps of the sensor were characterized and the gas sensing performances were evaluated. Further optimization work on the sensor is necessary, with the aims of lowering its power consumption and improving its sensing performance.

Acknowledgements

This work was supported by the LABEX MANUTECH-SISE (ANR-10-LABX-0075) of Université de Lyon, within the program "Investissements d'Avenir" (ANR-11-IDEX-0007) operated by the French National Research Agency (ANR).

References

- [1] G. Mattana, D. Briand, Recent advances in printed sensors on foil, *Mater. Today* 19 (2016) 88-99.
- [2] D. Briand, A. Oprea, J. Courbat, N. Bârsan, Making environmental sensors on plastic foil, *Mater. Today* 14 (2011) 416-423.

- [3] A. Oprea, J. Courbat, N. Bârsan, D. Briand, N.F. de Rooij, U. Weimar, Temperature, humidity and gas sensors integrated on plastic foil for low power applications, *Sens. Actuators, B* 140 (2009) 227-232.
- [4] S. Khan, L. Lorenzelli, R.S. Dahiya, Technologies for Printing Sensors and Electronics Over Large Flexible Substrates: A Review, *IEEE Sens. J.* 15 (2015) 3164-3185.
- [5] A. Vasquez Quintero, F. Molina-Lopez, E.C.P. Smits, E. Danesh, J. van den Brand, K. Persaud, A. Oprea, N. Barsan, U. Weimar, N.F. de Rooij, D. Briand, Smart RFID label with printed multisensor platform for environmental monitoring, *Flex. Print. Electron* 1 (2016) 025003.
- [6] J. Courbat, D. Briand, L. Yue, S. Raible, N.F. de Rooij, Drop-coated metal-oxide gas sensor on polyimide foil with reduced power consumption for wireless applications, *Sens. Actuators, B* 161 (2012) 862-868.
- [7] S. Vallejos, I. Gràcia, E. Figueras, J. Sánchez, R. Mas, O. Beldarrain, C. Cané, Microfabrication of flexible gas sensing devices based on nanostructured semiconducting metal oxides, *Sens. Actuators, A* 219 (2014) 88-93.
- [8] F. Molina-Lopez, D. Briand, N.F. de Rooij, All additive inkjet printed humidity sensors on plastic substrate, *Sens. Actuators, B* 166 (2012) 212-222.
- [9] S. Claramunt, O. Monereo, M. Boix, R. Leghrib, J.D. Prades, A. Cornet, P. Merino, C. Merino, A. Cirera, Flexible gas sensor array with an embedded heater based on metal decorated carbon nanofibres, *Sens. Actuators, B* 187 (2013) 401-406.
- [10] E. Danesh, F. Molina-Lopez, M. Camara, A. Bontempi, A. Vásquez Quintero, D. Teyssieux, L. Thiery, D. Briand, N. F. de Rooij, K. C. Persaud, Development of a New Generation of Ammonia Sensors on Printed Polymeric Hotplates, *Anal. Chem.* 86 (2014) 8951-8958.
- [11] J. Courbat, D. Briand, J. Wöllenstein, N.F. de Rooij, Polymeric foil optical waveguide with inkjet printed gas sensitive film for colorimetric sensing, *Sens. Actuators, B* 160 (2011) 910-915.
- [12] W. Shen, Properties of SnO₂ based gas-sensing thin films prepared by ink-jet printing, *Sens. Actuators, B* 166-167 (2012) 110-116.
- [13] A. Vilà, A. Gomez, L. Portilla, J.R. Morante, Influence of In and Ga additives onto SnO₂ inkjet-printed semiconductor, *Thin Solid Films* 553 (2014) 118-122.
- [14] M. A. Andio, P. N. Browning, P. A. Morris, S. A. Akbar, Comparison of gas sensor performance of SnO₂ nano-structures on microhotplate platforms, *Sens. Actuators, B* 165 (2012) 13-18.

- [15] W. Shen, Y. Zhao, C. Zhang, The preparation of ZnO based gas-sensing thin films by ink-jet printing method, *Thin Solid Films* 483 (2005) 382-387.
- [16] S. Das, V. Jayaraman, SnO₂: A comprehensive review on structures and gas sensors, *Prog. Mater. Sci.* 66 (2014) 112-255.
- [17] D. Kohl, Function and applications of gas sensors, *J. Phys. D: Appl. Phys.* 34 (2001) R125–R149.
- [18] B. Riviere, J.-P. Viricelle, C. Pijolat, Development of tin oxide material by screen-printing technology for micro-machined gas sensors, *Sens. Actuators, B* 93 (2003) 531-537.
- [19] C. Pijolat, G. Tournier, P. Breuil, D. Matarin, P. Nivet, Hydrogen detection on a cryogenic motor with a SnO₂ sensors network, *Sens. Actuators, B* 82 (2002) 166-175.
- [20] S. Sujatha Lekshmy, K. Joy, SnO₂ thin films doped indium prepared by the sol-gel method: structure, electrical and photoluminescence properties, *J. Sol-Gel Sci. Technol.* 67 (2013) 29-38.
- [21] J. Zhang, S. Wang, Y. Wang, M. Xu, H. Xia, S. Zhang, W. Huang, X. Guo, S. Wu, Facile synthesis of highly ethanol-sensitive SnO₂ nanoparticles, *Sens. Actuators, B* 139 (2009) 369-374.
- [22] Z. Bin, Y. Chenbo, Z. Zili, T. Chunmin, Y. Liu, Investigation of the hydrogen response characteristics for sol-gel-derived Pd-doped, Fe-doped and PEG-added SnO₂ nano-thin films, *Sens. Actuators, B* 178 (2013) 418-425.
- [23] L. F. Chepik, E. P. Troshina, T. S. Mashchenko, D. P. Romanov, A. I. Maksimov, O. F. Lutskaya, Crystallization of SnO₂ produced by sol-gel technique from salts of tin in different oxidation states, *Russ. J. Appl. Chem.* 74 (2001) 1617-1620.
- [24] L. P. Ravaro, D.I. dos Santos, L.V.A. Scalvi, Effect of pH of colloidal suspension on crystallization and activation energy of deep levels in SnO₂ thin films obtained via sol-gel, *J. Phys. Chem. Solids* 70 (2009) 1312-1316.
- [25] N. Bârsan, U. Weimar, Understanding the fundamental principles of metal oxide based gas sensors; the example of CO sensing with SnO₂ sensors in the presence of humidity, *J. Phys.: Condens. Matter* 15 (2003) R813-R839.
- [26] S.H. Hahn, N. Bârsan, U. Weimar, S.G. Ejakov, J.H. Visser, R.E. Soltis, CO sensing with SnO₂ thick film sensors: role of oxygen and water vapour, *Thin Solid Films* 436 (2003) 17-24.
- [27] A. Stanoiu, S. Somacescu, J.M. Calderon-Moreno, V.S. Teodorescu, O.G. Florea, A. Sackmann, C.E. Simion, Low level NO₂ detection under humid background and associated sensing mechanism for mesoporous SnO₂, *Sens. Actuators, B* 231 (2016) 166-174.